arXiv:cond-mat/0701616v2 [cond-mat.other] 8 Aug 2007

Transition from a two-dimensional superfluid to a one-dimensional Mott insulator

Sara Bergkvist and Anders Rosengren
Department of Theoretical Physics, Royal Institute of Technology, AlbaNova, SE-106 91 Stockholm, Sweden

Robert Saers, Emil Lundh, Magnus Rehn, and Anders Kastberg
Department of Physics, Umeå University, SE-90187 Umeå, Sweden

A two-dimensional system of atoms in an anisotropic optical lattice is studied theoretically. If the system is finite in one direction, it is shown to exhibit a transition between a two-dimensional superfluid and a one-dimensional Mott insulating chain of superfluid tubes. Monte Carlo (MC) simulations are consistent with the expectation that the phase transition is of Kosterlitz-Thouless (KT) type. The effect of the transition on experimental time-of-flight images is discussed.

Cold atomic gases in optical lattices provide a means to study many-body quantum phenomena that offers both versatility, precision, and control. These techniques allowed for the spectacular realization of the Mott transition by Greiner *et al.* [1], which has inspired numerous proposals for creating and detecting exotic quantum phases in such systems.

By manipulating the alignment and the polarizations of the laser beams that build up the optical lattice, the geometry of the lattice can be changed. The probability for tunneling can be adjusted by changing the separation between potential wells, or by simply varying the irradiance. In conjunction, this brings about the possibility of designing optical lattices where the probability for tunneling differs significantly between different directions, and where this difference in tunneling rates can be a control parameter. By allowing the atoms to tunnel only along one direction, one essentially has created a 2D lattice of 1D quantum gases. By allowing tunneling in two directions, an array of 2D systems is created [2].

The tunability allows to explore the crossover between different dimensionalities. Thus, with a properly chosen geometry, it should be possible to start off with high laser irradiance and thus with deep potential wells. This system will be a Mott insulator, where the number of particles per site is fixed to an integer and there is no phase coherence. By lowering the irradiance in one direction, increasing the tunneling probability, one should reach a point where tunneling becomes probable along just one direction. This would give us isolated 1D tubes, known as Luttinger liquids [3]. Decreasing the irradiance in a second direction, we expect to reach a point where there is a crossover from this to a system of 2D superfluids, and eventually one global 3D superfluid [4, 5, 6]. In this Letter, this dimensional crossover is addressed by quantum MC simulations of an anisotropic bosonic Hubbard model in two dimensions. We show how the model can be readily realized in experiment, and predict the outcome of absorption imaging on both sides of the transition.

System. – Consider a gas of bosonic atoms at zero temperature in a 2D, anisotropic optical lattice. The gas is described by the Bose-Hubbard Hamiltonian [7]

$$H = -\sum_i \left(t_x b^\dagger_{i_x,i_y} b_{i_x+1,i_y} + t_y b^\dagger_{i_x,i_y} b_{i_x,i_y+1} + h.c. \right) + \frac{U}{2} \sum_i n_i(n_i-1) - \mu \sum_i n_i, \quad (1)$$

where $i = (i_x, i_y)$; b_i, $b_i^\dagger$ are bosonic annihilation and creation operators, $n_i = b_i^\dagger b_i$, U the interaction strength, μ the chemical potential, and t_x, t_y the tunneling matrix elements in the Cartesian directions. The crossover from 2D to 1D behavior considered in this paper can be realized in a simple cubic optical lattice with a potential of the form $V(\mathbf{r}) = \sum_{\alpha=x,y,z} V_\alpha \cos^2 k\alpha$. If the potential barrier in the z direction V_z is strong enough, there can be no tunneling in the z direction, and the sample can be considered as a stack of independent 2D systems [2]. V_x should be chosen relatively weak in order to allow for superfluid flow in the x direction, and V_y is scanned over the physically interesting range. As will be shown, if the lattice has an extent of eight sites in the x direction there will occur a phase transition for $t_x/U = 0.3$ and $t_y/U \approx 6 \times 10^{-3}$. As an example, for a gas of ^{87}Rb atoms in an optical lattice with wavelength $\lambda = 850$ nm, these tunneling matrix elements are obtained by choosing potential strengths $V_x = 2.5E_{\rm rec}$, $V_y = 30E_{\rm rec}$, and $V_z = 80E_{\rm rec}$, where $E_{\rm rec}$ is the single-photon recoil energy for a wavelength of 780nm [1].

Phase diagram. – The Hubbard model exhibits a zero-temperature quantum phase transition from a superfluid to a Mott insulating state when the ratio of the tunneling matrix elements and the coupling strength, t_x/U and t_y/U, are decreased below a critical value [8]. In one dimension (i.e., either $t_x = 0$ or $t_y = 0$), it is known that the phase transition occurs at $t/U = 0.3$ for the system with an average of one particle per site [9]. For the anisotropic 2D model considered here, a mean-field argument implies that t should be replaced by the sum $t_x + t_y$ in the 1D expression, so the transition occurs when $(t_x + t_y)/U = 0.3$. For finite systems the phase transition occurs at a smaller value of t/U.

Consider the anisotropic case, where one of the tun-

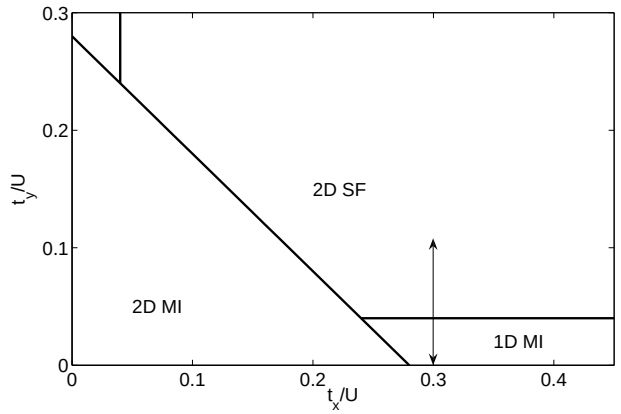

FIG. 1: Phase diagram for the finite anisotropic Hubbard model at number density $n = 1$. The 2D superfluid and Mott insulating phases are denoted by "2D SF" and "2D MI", respectively. The size of the 1D Mott insulating phase "1D MI" has been exaggerated in the figure. The vertical double arrow indicates the interval along which the MC calculations in this study have been performed.

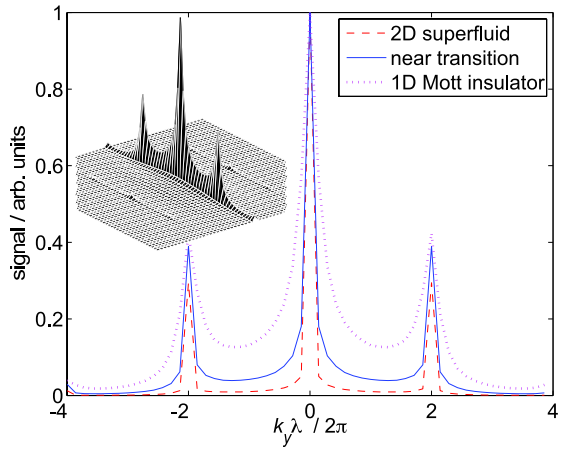

FIG. 2: Velocity distribution along the weakly coupled lattice direction. The curves corresponds to a ratio of the tunneling matrix element to the interaction strength, $t_y/U = 0.012$ (dashed line), 0.0025 (full), and 1.5×10^{-3} (dotted). The inset shows the full 2D profile of the velocity distribution for the case $t_y/U = 1.5 \times 10^{-3}$. The system size is 12×12 sites.

neling matrix elements, say, t_x, is larger than the critical 1D value and the other one, t_y, is varied. In an infinite 2D system, it is known that the system remains a 2D superfluid (2D SF) right down to the point where t_y vanishes [10]. In other words, when the coupling in one direction vanishes, the system can be seen as an array of uncoupled Luttinger liquids. However, any finite tunneling, no matter how small, will induce phase coherence between the Luttinger liquid tubes, so that an anisotropic phase, with superflow only in one direction, does not exist. However, the situation changes when the system is not infinite. If each Luttinger liquid has a finite length, there is an energy barrier against tunneling into and out of it, and as a result there exists, for small t_y, an anisotropic state with coherence only along the x direction [4, 5, 6]. Hence, when the weaker tunneling matrix element t_y is small enough, the state of the system is a 1D Mott insulator (1D MI), where each site is a Luttinger liquid tube extending along the x direction. If the tunneling t_y is increased above a critical value t_c, the tubes become phase correlated and the system undergoes a quantum phase transition to a superfluid state. In a geometry where the system is infinite in the weakly coupled direction, the state is an 1D SF, i. e., a superfluid chain of Luttinger liquids, just above the phase transition, but is expected to undergo a crossover into a 2D SF as the coherence length becomes smaller than the tube length L_x, and the picture of separate Luttinger liquid tubes can no longer be sustained. The crossover between 1D SF and 2D SF presumably happens over a very short interval, why we in the following shall speak of the 1D MI - 2D SF transition. In an actual experiment where the system is finite, there is a crossover between 1D MI and 2D SF without an intermediate 1D SF state. In the 1D MI phase, each tube along the x direction behaves as an independent Luttinger liquid, characterized by an (inverse) exponent K [3, 4, 5]. This so-called Luttinger parameter determines the algebraic decay of the single-particle correlation function $\Gamma(j)$, according to

$$\Gamma_x(j) \equiv \langle b^\dagger_{i_x,i_y} b_{i_x+j,i_y} \rangle \sim j^{-1/(2K_x)}. \qquad (2)$$

This form for the asymptotic behavior holds only in the 1D case, i. e., for decoupled Luttinger liquid tubes. Γ_y is defined analogously. The critical tunneling was in Refs. [4, 5, 6] found to depend on the parameters as

$$t_c \propto L_x^{-2+\frac{1}{2K_x}}. \qquad (3)$$

Since it is known that $K_x > 2$ here [9], the exponent in Eq. (3) is expected to be slightly less than -1.75. The constant of proportionality in Eq. (3) depends on the model used to integrate out the dynamics in the tubes as well as on the dimensionality. These phase boundaries have been indicated at arbitrarily chosen positions in the phase diagram in Fig. 1.

Experimental signal. – Detection of the transition can be achieved by applying an optical lattice potential, $V(\mathbf{r})$, to a Bose-Einstein condensate in a magnetic trap. Ramping up $V(\mathbf{r})$ adiabatically ensures that the atoms are not heated, and that they are loaded to the lowest energy band of the lattice [1]. For high lattice barriers, the correlations between wells are lost after some hold time, resulting in a Mott insulating state, whereas in the case of low barrier heights the sample stays coherent. The state of the system is detected by standard time of flight absorption imaging. When the sample is released by ramping down the lattice and magnetic trap non-adiabatically,

it will expand freely. The expansion reveals the sample's velocity distribution $n(\mathbf{k})$, given by the Fourier transform of the trapped sample density distribution in real space $n(\mathbf{r})$ [13], $n(\mathbf{k}) \propto |w(\mathbf{k})|^2 S(\mathbf{k})$, where the first part is the Fourier transform of the Wannier function for the first Bloch band $w(\mathbf{r})$, and the second part, the structure factor $S(\mathbf{k})$, is the Fourier transform of the correlation function $\Gamma(\mathbf{r})$ defined in Eq. (2). The structure factor has the periodicity $4\pi/\lambda$.

Knowing the structure factor from MC simulations (see below), and calculating the Wannier functions for a cubic lattice, a theoretical prediction for the actual experimentally observable time-of-flight profiles can thus be obtained. The result is shown in Fig. 2. The profile of the cloud in the direction of weak tunneling is determined by the state of the system. When distinct peaks are visible at $k = 0, \pm 4\pi/\lambda$, a 2D SF is detected. This is connected with a slow decay of the real-space correlation function $\Gamma(\mathbf{r})$. If the lattice depth is increased, the sample passes into the 1D MI and the interference fringes are blurred as $\Gamma(\mathbf{r})$ becomes exponentially decaying. The signal would be even more pronounced for a larger system. However, the peaks will be visible far into the Mott insulator regime, an effect caused by maintained short-range coherence [13].

Method. – To solve for the ground state of the Bose-Hubbard model, Eq. (1), Quantum MC calculations with the stochastic series expansion algorithm are used [11, 12]. We simulate a system of size $L_x \times L_y$ lattice sites with periodic boundary conditions to minimize edge effects. The inverse temperature is $\beta = (k_B T)^{-1} = 1000 U^{-1}$; this is large enough to ensure that the system is in its ground state. The results presented in the article are calculated with a fixed $t_x = 0.3U$ with t_y/U being varied across the anticipated phase transition as indicated by the double arrow in Fig. 1. Trial calculations not shown here, using larger values of t_x/U, have yielded similar results. The calculations have been performed at the fixed average number of particles per site $n = 1$.

Transition. – To locate the 2D SF↔1D MI transition, three different observable quantities are calculated, each of which can be considered a measure of superfluidity. The superfluid density, ρ_s, is readily obtained from the simulation data as $\rho_s = \langle W_y^2 \rangle / \beta$, where W_y^2 is the so-called square winding number in the y direction, defined as the squared net number of times a particle crosses the periodic boundary in the calculations [14]. Second, the off-diagonal correlation function along the y direction, $\Gamma_y(j)$, is, as we have seen, experimentally accessible through the momentum distribution, which is closely related to its Fourier transform. We now study the correlation function in real space evaluated at half the system size, $\Gamma_y(y = L_y/2)$ which we expect to behave differently above and below the transition. Above, $\Gamma_y(y)$ decays algebraically, below exponentially. A third observable is the compressibility, defined as the mean of variances,

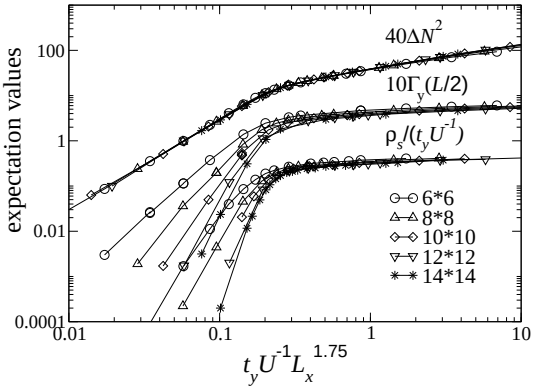

FIG. 3: From top to bottom, the density fluctuation, the correlation, and the superfluid density are shown as a function of the size-independent parameter $t_y L_x^{1.75}/U$, for different system sizes $L_x \times L_y$ measured in lattice sites, as indicated in the legend. The scale is logarithmic on both axes. The correlation function and the compressibility are multiplied by arbitrarily chosen numerical factors to separate the three groups of lines. The superfluid density is divided by the tunneling matrix element for better visual clarity.

$\Delta N^2 = \sum_{i_y} \mathrm{var}\left(\sum_{i_x} n_{i_x,i_y}\right)/L_y$. It is expected that ΔN^2 changes its behavior at the transition: due to the finite length of the tubes, the fluctuations in the number of particles per tube will be suppressed once the system becomes insulating in the weakly coupled y direction.

In Fig. 3, the three quantities, ρ_s, $\Gamma_y(L_y/2)$, and ΔN^2, are shown for lattices $6 \le L_x = L_y \le 14$. The observables are plotted as functions of $t_y L_x^{1.75}/U$. The exponent of L_x is given by Eq. (3) and the value of K_x is determined by a finite-size scaling of the superfluid density as explained below. For a system with $t_x/U = 0.4$, not shown here, the best scaling is obtained for $t_y L_x^{1.79}/U$. The superfluid density in the y direction is in the superfluid phase seen to be approximately proportional to the coupling constant t_y/U, hence the superfluid density is divided by t_y/U. It is clear from Fig. 3 that there is a change in behavior around $t_y/U \approx 0.3 L_x^{-1.75}$. The three quantities in Fig. 3 are behaving as in a 1D MI-SF transition. The true 1D system can be obtained by putting $L_x = 1$ and letting $L_y \to \infty$, and we then recover the known value for the true 1D transition $t_y/U = 0.3$ [9]. (The same curves are obtained for $L_y > L_x$, but these data are not shown here not to overload the figure). The finite size effects above the transition point are taken care of by scaling L_x with the power 1.75. If the curves instead were plotted as a function of t_y/U, they would not tend to coincide.

Since in the critical region, the system can be described as a 1D chain of Luttinger liquid tubes, the phase transition is a 1D quantum phase transition. Such a transition can be mapped onto a classical phase transition in 2D [15], and if the number of particles is held fixed as in the

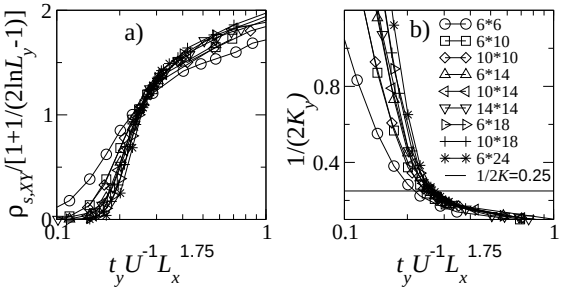

FIG. 4: a) Superfluid density in the dual XY model, Eq. (4), scaled according to Weber-Minnhagen scaling. b) Exponent of the algebraic decay of the correlation Γ_y, as a function of the dimensionless coupling parameter $t_y L_x^{1.75}/U$. The horizontal line shows the critical value expected for a 1D Mott transition at fixed density, $1/(2K) = 0.25$. Different curves correspond to different system sizes; the same symbols are used in both parts of the figure.

present study, it is known that the transition considered here is a KT transition [8].

Characteristic for such a transition is a discontinuous jump of the superfluid density at the critical point [14]. In Fig. 4 a) a finite size scaling of the data for the superfluid density is illustrated. In order to do the scaling, a series of mappings has to be performed: First, according to Ref. [4], the original Hubbard model can be rewritten as a Josephson junction chain model, where each Luttinger liquid tube is treated as a site, with a charging energy $E_C \propto L_x^{-1}$ and hopping energy $E_J \propto t_y L_x^{1-1/2K_x}$. Next, this model is in turn mapped onto a 2D XY-model if one identifies $\beta_{XY} = \sqrt{E_J/E_C}$, $L_{x,XY} = \beta\sqrt{E_J E_C}$, and $L_{y,XY} = L_y$ [15], where the quantities referring to the dual 2D XY-model carry the subscript XY. As a result, the superfluid density in the 2D XY-model is [14]

$$\rho_{s,XY} \propto \langle W_y^2 \rangle L_y/\beta t_y L_x^{1-1/2K_x}. \qquad (4)$$

The quantum phase transition occurring at a critical tunneling in the underlying Hubbard model corresponds to the well-known finite-temperature KT transition in the 2D XY-model. According to Weber-Minnhagen scaling [16], $\rho_{s,XY}$ should be proportional to $1 + 1/(2\ln L_y + C)$ at the critical point, where C is a fitting constant to be determined. The quantity $\rho_{s,XY}$ divided by this function should therefore assume the same value for all system sizes at the critical point, if C and K_x are chosen correctly. The best scaling is obtained with $C = -1$ and $K_x = 2$ and is shown in Fig. 4 a). The scaling behavior supports the conclusion that the transition is a KT transition and the critical point is $t_c/U \approx 0.27 L_x^{-1.75}$.

An independent method for calculating the location of the transition is provided by fitting the correlation function in the y-direction, Γ_y, to an algebraic decay function according to Eq. (2). The phase transition for a 1D Hubbard model at a fixed number of atoms per site is found by determining the point where the exponent in the power law, $1/(2K_y)$, becomes equal to 0.25 [9].

In Fig. 4 b) the exponent obtained from an algebraic fit is displayed for different system sizes. There is a clear finite-size effect, the larger L_y the larger the critical value. The critical point at which $1/(2K_y) = 0.25$ for the infinite system is determined to be $t_c/U \approx 0.3 L_x^{-1.75}$, in agreement with the scaling in Fig. 4 a) and the point of loss of superfluidity observed in Fig. 3.

Summary – We have reported theoretical evidence for a transition in a 2D Hubbard model between a 2D superfluid and a 1D Mott insulating state consisting of isolated 1D tubes. The location of the transition is consistent with predictions based upon a random phase approximation made in Refs. [4, 5, 6]. By scaling it is shown that the system undergoes a KT transition. The transition can be induced using atoms in an optical lattice and observed by time-of-flight imaging.

This work was supported by the Göran Gustafsson foundation, the Swedish Research Council, the Knut and Alice Wallenberg Foundation, the Carl Trygger foundation, and the Kempe foundation.

[1] M. Greiner, O. Mandel, T. Esslinger, T. Hänsch, and I. Bloch, Nature **415**, 39 (2002).
[2] M. Köhl, H. Moritz, T. Stöferle, C. Schori, and T. Esslinger, J. Low Temp. Phys. **138**, 635 (2005).
[3] T. Giamarchi, *Quantum Physics in One Dimension* (Clarendon, Oxford, 2004).
[4] A. F. Ho, M. A. Cazalilla, and T. Giamarchi, Phys. Rev. Lett. **92**, 130405 (2004).
[5] M. A. Cazalilla, A. F. Ho, and T. Giamarchi, New J. Phys **8**, 158 (2006).
[6] D. Gangardt, P. Pedri, L. Santos, and G. Shlyapnikov, Phys. Rev. Lett. **96**, 040403 (2006).
[7] D. Jaksch, C. Bruder, J. I. Cirac, C. W. Gardiner, and P. Zoller, Phys. Rev. Lett. **81**, 3108 (1998).
[8] M. P. A. Fisher, P. B. Weichman, G. Grinstein, and D. S. Fisher, Phys. Rev. B **40**, 546 (1989).
[9] T. D. Kühner, S. R. White, and H. Monien, Phys. Rev. B **61**, 12474 (2000).
[10] K. B. Efetov and A. I. Larkin, Sov. Phys.–JETP **39**, 1129 (1974).
[11] A. W. Sandvik, Phys. Rev. B **59**, R14157 (1999).
[12] O. Syljuåsen and A. W. Sandvik, Phys. Rev. E **66**, 046701 (2002).
[13] F. Gerbier, A. Widera, S. Fölling, O. Mandel, T. Gericke, and I. Bloch, Phys. Rev. Lett. **95**, 050404 (2005).
[14] R. G. Melko, A. W. Sandvik, and D. J. Scalapino, Phys. Rev. B **69**, 014509 (2004).
[15] S. L. Sondhi, S. M. Girvin, J. P. Carini, and D. Shahar, Rev. Mod. Phys. **69**, 315 (1997).
[16] H. Weber and P. Minnhagen, Phys. Rev. B **37**, 5986 (1988).